Physicochemical Characterization of Maize Tassel as an Adsorbent. I. Surface Texture, Microstructure, and Thermal Stability

Caliphs M. Zvinowanda,[1] Jonathan O. Okonkwo,[1] Nana M. Agyei,[2] Pride N. Shabalala[1]

[1]*Department of Environmental, Water, and Earth Sciences, Tshwane University of Technology, Private Bag X680, Arcadia, Pretoria 0001, South Africa*
[2]*Department of Chemistry, University of Limpopo, P.O. Box 235, Medunsa 0204, South Africa*

ABSTRACT: In this study, various physicochemical parameters were evaluated for maize tassel, a novel adsorbent. The Brunauer–Emmett–Teller (BET) isotherm was used to experimentally model N_2-adsorption data (up to a relative pressure of 0.30); the results indicated that the powdered material was mesoporous with a BET specific surface area, total pore volume (up to a relative pressure of 0.98), and average pore width (4V/A by BET) of 2.52 m^2/g, 0.0045 cm^3/g, and 7.2 nm, respectively, for the 150–300-μm fraction. Laser diffraction pattern analysis yielded particle size distributions for the 45–50-, 50–150-, and 150–300-μm fractions. High-reso- lution scanning electron microscopy revealed a microstructure showing predominantly flattish, rodlike particles. The material exhibited stability to thermal decomposition up to about 230°C, as evidenced by the results obtained from si- multaneous thermogravimetry/differential thermal analysis and differential scanning calorimetry. © 2008 Wiley Periodicals, Inc. J Appl Polym Sci 111: 1923–1930, 2009

Key words: adsorption; differential scanning calorimetry (DSC); electron microscopy; microstructure; particle size distribution

INTRODUCTION

Research efforts in water, wastewater, and effluent treatment have focused to a large extent on the re- moval of heavy metals because of their well-known toxicity. Technologies that have been developed for the removal of these metals from aqueous solutions involve processes such as ion exchange, reverse os- mosis, membrane filtration, sludge leaching, electro- winning, solvent stripping, precipitation, and adsorption. Adsorption is the predominant process, and commercial activated carbon (CAC) has been the most successful adsorbent investigated and used for this purpose.[1–5]

However, the adsorptive removal process is rela- tively expensive when a pure adsorbent such as CAC is used. This fact has led to ongoing research into the feasibility of using lower cost adsorbents as alternatives to CAC for removing heavy metals and other pollutants from aqueous solutions. Materials that have been investigated in this respect include zeolites,[6] chitosan,[7] clays,[8] natural oxides,[9] saw- dust,[10] rice husks,[11] coal fly ash,[12] and lignite.[13]

The ideal candidate is a low-cost adsorbent that not only is readily available in large quantities locally but also is otherwise discarded as waste. Tas- sel, the male inflorescence of the maize plant, which forms at the top of the stem, evidently meets these requirements. It is discarded by local communities in South Africa and elsewhere in huge quantities with the rest of the plant once the cobs have been harvested. The authors have not yet found any infor- mation in the literature regarding the physical char- acteristics or chemical composition of tassel. Being a fibrous part of a plant that is rich in carbohydrates, it is expected to contain a high proportion of poly- saccharides with cellulosic surface hydroxyl groups that can bind metal cations. There might be a lot of lignin in the dried maize tassel, and lignin might also contribute to the adsorption of metal ions.

It is important to characterize a candidate adsorbent because how efficiently an adsorbent can perform is influenced fundamentally by its inherent physico- chemical characteristics. Furthermore, the sorption capacity of natural biosorbents often requires enhance- ment through physical and chemical modification, and successful modification requires knowledge of their morphology (texture and microstructure) and surface

chemistry. Researchers in the field characterize the texture of adsorbents by evaluating parameters such as the porosity and surface area/particle size; techniques such as N_2 sorptiometry[14–16] and laser diffraction analysis[8,17] have been used in this respect. SEM is the method of choice that has been commonly used to characterize the microstructures of adsorbents.[18,19,20] Thermal analysis and calorimetry often yield information on properties that have an impact on the surface morphology and sorptive behavior, such as thermal stability, hydroscopic water, volatiles, and phase transitions during pyrolysis,[21,22] and can therefore be used in adsorbent sorption capacity optimization.

The surface area and porosity are two of the most important properties of a material being developed into an adsorbent. Textural characterization of the following carbonaceous materials prepared from natural adsorbents has been reported: cotton stalks,[23] plum kernels,[24] corncobs,[25] bagasse,[26] peanut hulls and nutshells,[27] and olive stones.[28] Generally, the more porous the material is, the larger the surface area is and hence the greater the adsorption capacity is. The adsorptive capacity of an adsorbent depends also on its surface chemistry functionality, a property that is usually predominant in cationic removal from aqueous systems.

This study was aimed at determining various physicochemical characteristics of maize tassel, an agrowaste material that has exhibited a very commendable potential not only for the adsorptive removal of heavy metals from aqueous[29] and organic systems but also for possible utilization as a filler material for plastic products. The research will eventually have an impact on the economy of African communities and farmers, for whom maize is the main staple, by creating small-scale businesses.

EXPERIMENTAL

Material

The tassel was sampled from hybrid cultivar SC71105, a maize variety bred by SEED-CO (Masvingo, Zimbabwe). The material was first air-dried for 7 days and then thoroughly rinsed with copious amounts of distilled water. The material was then placed in an air-powered drying hood to remove dripping water. Finally, the tassel was dried in an oven with the temperature set at 105°C for 24 h to expel any moisture present. The dried material was then milled with hammer mill a Laboratory Mill 3100 (Marisburg, South Africa) with stainless steel blades mounted with a 500-μm sieve. A coarse powder of variable particle size was generated and was further fractionated into the following particle size ranges: 45–50, 50–150, 150–300, 300–500, 300–560, 560–630, and 630–750 μm. Stacks of analytical sieves

of specification ISO3310-1 were used to accomplish the fractionation. The second, third, and fourth fractions were the most abundant.

Surface characterization

Nitrogen adsorption–desorption isotherms

The porosity and specific surface area were determined by the modeling of N_2-adsorption data with the Brunauer–Emmett–Teller (BET) isotherm. The particle size distribution was determined by the fitting of an algorithm to patterns generated by the diffraction of a laser beam by suspended adsorbent particles. A surface area and porosity analyzer (ASAP 2020 V3.00H, Micromeritics Instrument Corp., Norcross, GA) was used to perform textural analysis. The nitrogen used for this purpose was instrument-grade. Textural characteristics of the tassel powder were determined by nitrogen adsorption–desorption at an analysis bath temperature of $-197°C$ with a warm free space of 16.8 cm^3 and an equilibration interval of 10 s. The sample was automatically degassed. The saturation pressure (P_0) was calculated from the temperature options dialog box of the computer control system, and a value of 655.8 mmHg was used. A sample mass of 0.200 g was placed in a cold free space holder of 52.6 cm^3, and the adsorptive properties of nitrogen were analyzed at a maximum manifold pressure of 925 mmHg. The adsorption–desorption isotherm, the BET surface area, the single-point adsorption total pore volume, and the desorption average pore width were determined.

Measurement of the BET surface area

P_0 of an adsorbent is the pressure by which the surface is completely covered by the adsorbate material. In surface area analysis, a commonly used parameter in BET isotherms is the relative pressure (P/P_0).

For points taken before the P_0 measurement, we can be used the following equation:

$$P_{01} = P_{0i} + [(P_{02} - P_{0i}) \times (T_1 - T_{01})/(T_{02} - T_{01})] \quad (1)$$

where P_{01} is the saturation pressure before the Ith data point (mmHg), P_{0i} is the most recently measured saturation pressure before the Ith data point (mmHg), P_{02} is the first measured saturation pressure after the Ith data point (mmHg), T_1 is the time when the Ith data point is taken (min), T_{01} is the time at which P_{01} is measured (min), and T_{02} is the time at which P_{02} is measured (min). With this equation, we can calculate the relative pressure of the Ith data point [P_{rel1} [(mmHg)]:

$$P_{rel1} = P_1/P_{0I} \quad (2)$$

where P_{0I} is the saturation pressure for the Ith data point (mmHg) and P_1 is the absolute pressure for the Ith data point taken at equilibrium (mmHg).

Calculation of the BET surface area

To calculate the BET surface area, the volume of adsorbed N_2 gas needs to be known. The volume adsorbed for the Ith dose is calculated as follows:

$$V_{gas1} = V_{gasI-1} + V_{LOW} \times [(P_{sys11}/T_{sys11})$$
$$- (P_{sys21}/T_{sys21})] \times T_{STD}/P_{STD} \qquad (3)$$

$$V_{ads1} = V_{gas1} - P_{sam1} \div P_{STD}$$
$$\times (V_{FC} + P_{sam1} \times V_{ABT} \times C) \qquad (4)$$

$$Q_1 = V_{ads1}/W_{asm} \qquad (5)$$

where C is the nonideality correction factor, P_{sam1} is the sample pressure after equilibrating the Ith dose of gas onto the sample (mmHg), P_{STD} is the standard pressure (760 mmHg), P_{sys11} is the system manifold pressure before the Ith dose of gas onto the sample (mmHg), P_{sys21} is the system manifold pressure after the Ith dose of gas onto the sample (mmHg), Q_1 is the amount of gas adsorbed per gram of the sample (cm^3/g STP), T_{STD} is the standard temperature (273.13 K), T_{sys11} is the system manifold temperature before the Ith dose of gas onto the sample (K), T_{sys21} is the system manifold temperature after the Ith dose of gas onto the sample (K), V_{ads1} is the amount of gas adsorbed after equilibrating the Ith dose (cm^3 STD), V_{ABT} is the portion of cold free space at the analysis bath temperature used in the nonideality correction (cm^3 at standard temperature), V_{FC} is the volume of cold free space (cm^3 at the standard temperature), V_{gas1} is the total amount of gas dosed into the sample tube after the Ith dose (cm^3 STP), V_{gasI-1} is the total amount of gas in the sample tube after the $I - 1$th dose (cm^3 STP), V_{LOW} is the low manifold volume (cm^3), and W_{sam} is the weight of the sample (g). For each point designated for surface area calculations, the BET[2] transformation [B_1 (g/cm^3 STP)] can be calculated as follows:

$$B_1 = P_{rel1}/[(1.0 - P_{rel1}) \times V_{ads1}] \qquad (6)$$

If a least-square fit is performed on the (P_{rel1}, B_1) designated pairs, where P_{rel1} is the independent variable and B_1 is the dependent variable, the following can then be calculated:

1. Slope [S (g/cm^3 STP)].
2. y intercept [Y_{INT} (g/cm^3 STP)].
3. Error of S (g/cm^3 STP).
4. Error of Y_{INT} (g/cm^3 STP).
5. Correlation coefficient.

Using the results of the aforementioned calculations, we can calculate the BET surface area [SA_{BET} (m^2/g)] and BET C value:

$$SA_{BET} = CSA \times (6.023 \times 10^{23})/[(2.2414 \text{ cm}^3 \text{ STP})$$
$$\times (10^{18} \text{ nm}^2/\text{m}^2) \times (S + Y_{INT})] \qquad (7)$$

$$C = (S + Y_{INT})/Y_{INT} \qquad (8)$$

where CSA is the analyzed gas molecule cross-sectional area (nm^2).

From eq. (7), the volume of the monolayer [V_M (cm^3/g STP)] can then be calculated as follows:

$$V_M = 1/(C \times Y_{INT}) = 1/(S + Y_{INT}) \qquad (9)$$

The BET surface area plot is linear in the P/P_0 range of 0–0.3 for the following equation:

$$P/P_0 = k/[Q(P_0/P - 1)] \qquad (10)$$

where k is the proportionality constant and Q is the quantity of N_2 adsorbed (cm^3/g STP). During the analysis, the values of P/P_0 and Q were recorded as functions of the elapsed time. The analysis bath temperature was calculated from the values. A measurement interval of 120 min was used for these analyses. The analyses were given an equilibration time ($P/P_0 = 1.00$) of 10 s and a minimum equilibration delay time of 600 s.

The pore shape is mainly unknown, but it could be estimated by a model. Three basic models exist: cylindrical pores, which are circular in cross section; ink-bottle pores, which have a narrow neck and wide body; and slit-shaped pores with parallel plates. In this study, pore volumes and pore sizes were determined to establish the most suitable model for describing the structure of tassel pores.

Particle size analysis

Particle size analysis was performed with a Saturn Digisizer 5200 VI.II (Micromeritics Instrument) and a Mastersizer 2000, version 2.000 (Malvern Instruments, Ltd., Malvern, United Kingdom). Various tassel fractions were analyzed to determine their particle size distribution. Two grams of the material was suspended in water and then ethanol as a background material with a few drops of 1.0% Triton X added as a dispersant, and it was pumped past a laser beam. Laser diffractometry principles were used, an algorithm being applied to the data collected by the computer to calculate the parameters of interest. The cumulative particle diameters were measured at $d(0.1)$, $d(0.5)$, and $d(0.9)$, that is, for 10, 50, and 90% of the particles.
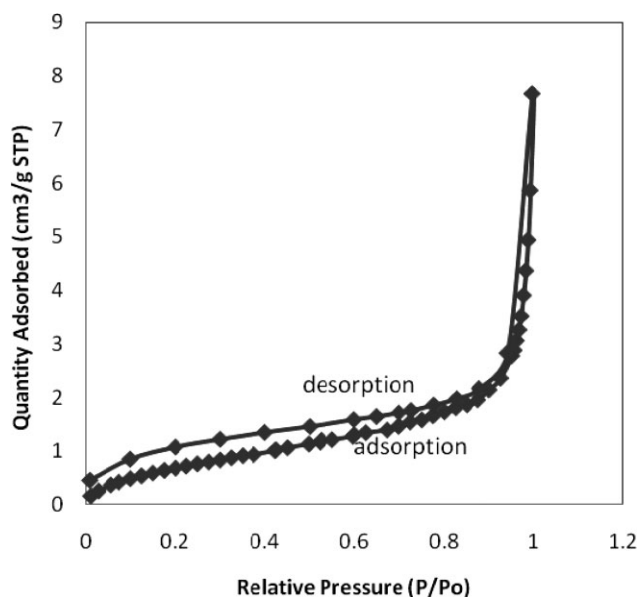
Figure 1 Adsorption–desorption curve for a 45–50-μm particle size tassel.

High-resolution scanning microscopy analysis (HRSEM)

The microstructure was determined with a TSM-6000F scanning electron microscope (JEOL, Tokyo, Japan). Various fractions of tassel powder in their natural state with sizes ranging from 45 to 750 μm were morphologically characterized by high-resolution field emission scanning electron microscopy.

Thermogravimetry (differential thermogravimetry)/ differential thermal analysis [TG (DTG)–DTA] and differential scanning calorimetry (DSC) analyses

A simultaneous TGA/sDTA 851 thermal analyzer (Star System, Mettler–Toledo, Hague, Switzerland) linked to a TSO 801 robotic sampler and a TSO 800 GCI gas control unit and a DSC Q20 V23.10 Build 79 scanning calorimeter (Universal V4.4A, TA Instruments, Binghamton, NY) were used for thermal analysis. Samples and reference material were heated in a 70.0-μL alumina pan made of aluminum oxide. Simultaneous TG (DTG)–DTA analysis in air was performed by the placement of a 15.5-mg sample or material into the sample pan, which was then heated in a dynamic mode from 25 to 900°C at a heating rate of 10°C/min and an air flow rate of 50 mL/min. In the DSC analysis, a sample of 2.00 mg was placed in an aluminum pan and heated with a ramp of 10°C/min and a nitrogen flow rate of 50 mL/min over a temperature range of 25–450°C. The DSC analysis was repeated after drying of the tassel powder for 24 h at 105°C in an oven.

RESULTS AND DISCUSSION

Surface texture

Figure 1 shows the nitrogen adsorption–desorption isotherm measured at −196°C. The isotherm of the tassel adsorbent is characteristic of materials without micropores because the adsorption hysteresis present indicates mesoporosity characteristics. The adsorption–desorption curve of the tassel is a typical type IV linear plot because it exhibits a hysteresis loop as the desorption curve lags behind the adsorption curve.[30] The plot further corroborates the evidence that this adsorbent is mesoporous in nature.

The plot of P/P_0 as a function of the inverse of the molar fraction adsorbed gives a linear curve with a correlation coefficient of 0.9987, a BET surface area of 2.82 ± 0.042 m^2/g, a slope of 1.47 ± 0.022 g/cm^3 STP, a y intercept of 0.075 ± 0.0040 g/cm^3 STP, a C value of 20.6, a maximum quantity of nitrogen adsorbed (Q_m) value of 0.648 cm^3/g STD, and a molecular cross section of 0.162 nm^2 (Fig. 2). The region signifies the monolayer adsorption of the sorbate, presenting a linear curve. The regression value shows that the adsorption of nitrogen on the adsorbent is in agreement with theoretical work in which P/P_0 is expected to be proportional to the molar fraction of adsorbed nitrogen for P/P_0 between 0 and 0.30. Above $P/P_0 = 0.30$, the pores are filled, and the development of adsorbate multilayers on the surface adsorbent occurs, resulting in the sigmoidal shape of the isotherms.[31] The adsorption capacity of these materials, which are still under development, is highly promising.

Table I shows a summary of the physical parameters of the two tassel fractions that were analyzed
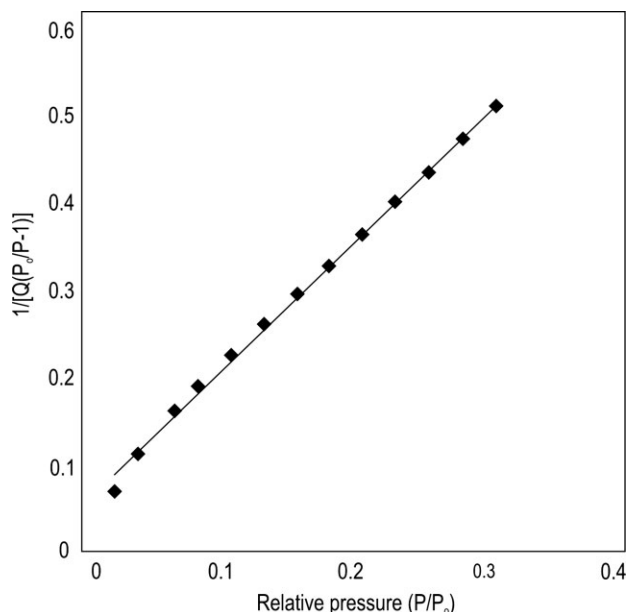

Figure 2 BET surface area plot for $P/P_0 = 0$–0.30.

TABLE I
Adsorption Parameters Obtained by the Application of the BET Model to Adsorption Isotherms of Nitrogen at −196°C

Particle size range (μm)	Surface area $(m^2/g)^a$	S_{BET} $(m^2/g)^b$	Pore volume $(cm^3/g)^c$	Pore size (nm)
150–300	2.22	2.52	0.00453	7.2
45–50	2.54	2.82	0.00604	8.6

[a] $P/P_0 = 0.30$.
[b] $P/P_0 = 0.98$.
[c] $4V/A$ by BET.

TABLE II
Variation of the Particle Diameter with the Background Material

Particle range (μm)	Particle diameter (μm)			Specific surface area (m^2/g)
	$d(0.1)$	$d(0.5)$	$d(0.9)$	
50–150a	13.8	63.3	152	0.234
50–150w	21.0	84.4	204	0.165
150–300a	63.8	179	461	0.076
150–300w	36.5	160	431	0.107
300–500a	90.3	285	644	0.0523
300–500w	47.8	189	436	0.0886

a = alcohol; w = water.

for textural characteristics. The monolayer surface area and BET specific surface area (S_{BET}) of the tassel found in this investigation are almost comparable. These figures are very low in comparison with other known microporous adsorbents.[28,31,32,33] In our previous publication,[29] the uptake of Pb(II) in aqueous solutions by tassel was up to 87%, and an uptake of 30% by maize cob powder has been reported.[34] The adsorption of metals such as Cd(II), Cu(II), Ni(II), Pb(II), and Zn(II) has even shown how valuable maize wastes can be for metal pollution remediation.[35] BET textural properties of natural adsorbents such as carbonized avocado[32] and fly ash[12,36] have been determined. The avocado adsorbent had very large S_{BET} values (143–1069 m^2/g) and pore volumes (0.073–1.053 cm^3/g) versus S_{BET} for fly ash (2.50–19.0 m^2/g). The high sorption capacity of tassel[29] can probably now be attributed more to chemisorption than physisorption. A Fourier transform infrared analysis of tassel has shown that it has functional groups such as —OH, —CO, and NH$_2$ on its surface (results not presented here).

The pore width is used to classify adsorbent materials as microporous (<2 nm), mesoporous (2–50 nm), or macroporous (>50 nm).[30,37] The two maize tassel fractions analyzed in this study had average pore sizes of 7.2 and 8.5 nm. The monolayer surface area and the BET surface area for both analyzed particles are in the same range. The results show that there was insignificant multilayer formation. Other materials that have been analyzed, such as silica (300 m^2/g) and carbon black (960 m^2/g),[31] have significantly large S_{BET} values. These materials do not form a monolayer, which is essential for reversible adsorption–desorption processes. These materials are difficult to regenerate for subsequent use. Furthermore, this shows that the tassel adsorbent is a mesoporous solid. Mesoporous materials are known to have lower pore volumes than microporous materials.

The results of particle size analysis are shown in Table II. These results of particle diameter measurements in water and alcohol as dispersing liquids show no significant (95% confidence level) liquid

effect during the measurement process. The variation of the particle diameter was random. Fifty percent of the particles in each range had the average diameter. However, in each range, there existed a small percentage on either side of the lower or upper ranges. The particles of the smaller diameters have the potential to influence the sorption behavior of the adsorbent. The finer particles provide a significantly larger surface area than an equivalent weight of larger particles. This deduction is supported by the specific surface area of the particles as measured by the laser aberration algorithm.

The finer details of the particle size distribution of adsorbent fractions A, B, and C, which were analyzed, are shown in Figure 3. Each fraction has finer particles in the range of 1–10 μm, and they are almost equally distributed in the portions. The small
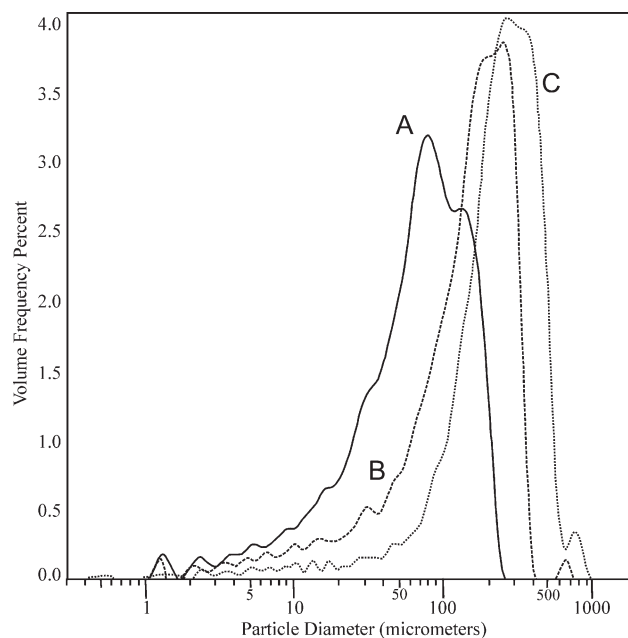
Figure 3 Volume frequency as a function of the particle diameter: (A) 50–150, (B) 150–300, and (C) 300–500 μm. The finer particles (A) as compared to B and C, have a large volume percent under the curve, which means they have a large surface area available for adsorption.
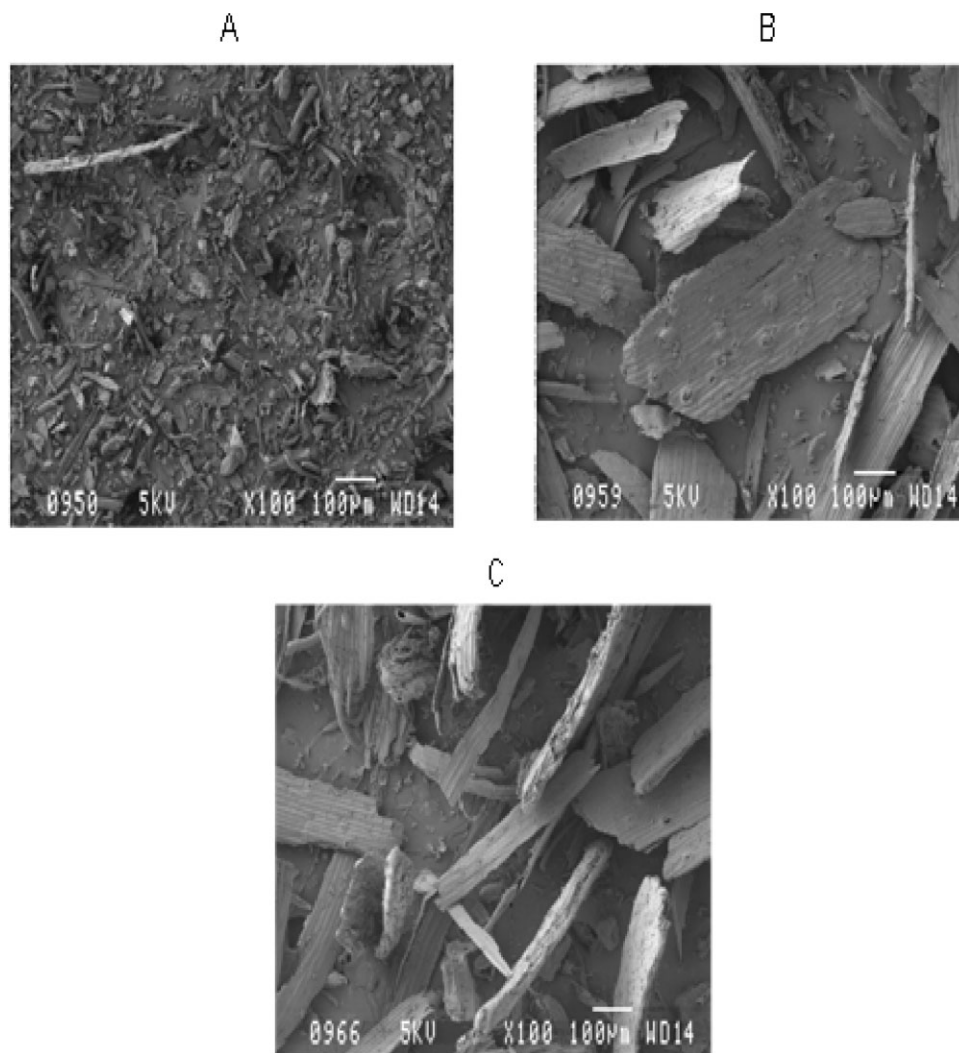
Figure 4   Micrographs of tassel fractions: (A) 50–150, (B) 150–300, and (C) 300–500 μm.

percentage of particles between 1 and 10 μm in size may have some significant influence on the adsorption capacity of tassel. Thus, materials having this range of particle size diameters are known to show increased adsorption capacity due to an increased specific surface area.[26]

Microstructure

The micrographs in Figure 4(A–C) exhibit flattish shapes originating from the fibrous nature of the tassel material. Minimum porosity is observed from the particles, so their adsorption behavior may be linked to their surface chemical morphology. The particles in the three micrographs exhibit random morphology associated with the method of preparation. The finer particles [Fig. 4(A)] show some degree of porosity versus the coarser ones [Fig. 4(B,C)].

Thermal stability

A thermal stability study of an adsorbent is very critical during product development stages. The ma-

terial will undergo pyrolysis resulting in physical and chemical transformation. During the heating program, the material absorbs energy supplied without its temperature being increased. Endothermic reactions in cellulosic materials usually result in the generation of noncombustible gases, primarily water vapor, with traces of carbon dioxide, glyoxal, and formic and acetic acids. At this stage, the material is dehydrated. Similar studies have shown that wood materials exhibit endotherms in two temperature ranges: below 200°C and from 200 to 280°C.[38] The dehydration process will result in an overall volumetric decrease of the tassel and a decrease in the cell cavity volume. Its activity can be improved by its subjection to an optimum heating program, which improves its porosity and surface functionality. The material will become more porous as volatile materials evolve from the matrix. These will lead to the formation of surface-active functional groups such as carbonyls and thiols with a high affinity for metal ions and other organic dyes. Thermal stability
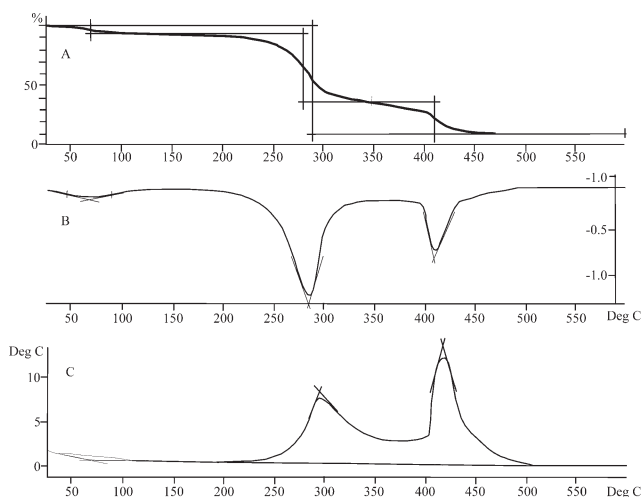
Figure 5 (A) TG, (B) DTG, and (C) DTA curves for tassel powder in air.

Figure 6 DSC curve for nondried tassel powder.

studies of cellulose have shown that it undergoes at least four thermal events when subjected to heating up to temperatures above 500°C.[39]

A simultaneous TG (DTG)–DTA analysis of tassel powder gave the curves shown in Figure 5. The DSC curves in Figures 6 and 7 show positive peaks as the heat flow to the sample is increased. Hence, the reactions taking place in this region result in the release of heat (exothermic reactions) from the sample, producing an exotherm. From the data obtained, the endotherms, exotherms, and plateaus may be interpreted as follows. The endotherm from 32 to 122°C [Fig. 5(B)] should be associated with a loss of volatiles and hydroscopic water. The bimodal exotherm with peaks at 303 and 429°C [Fig. 5(C)] and the plateau between them can be attributed to mixed reactions. These reactions include pyrolysis of various cellulosic macromolecules such as cellulose, pectins, and hemicellulose, which then undergo thermally catalyzed pyrolysis, forming more stable compounds that are richer in carbon. On further heating to temperatures above 405°C, they begin to char off, releasing combustible volatile gases that ignite to leave the ash. An analysis of the TG data for this study yielded an ash residue of about 9%. Similar materials such as wood cellulose have been reported to give a residue of about 10%,[37] which is in good agreement with the results obtained in this study.

Figures 6 and 7 show the DSC curves for the nondried and dried materials. Nondried tassel gave a larger endotherm (with a maximum at 89°C) than dried powder, which gave a poorly resolved endotherm (with a maximum at 67°C). The endotherm is a result of negative heat flow as the temperature applied to the sample is increased. This means that the internal processes taking place in the material
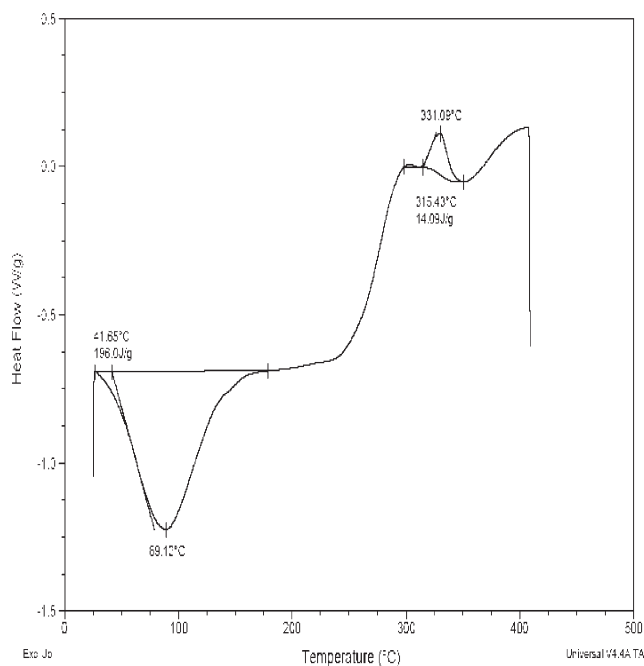
require energy; that is, they are endothermic processes. The larger endotherm observed in Figure 7 is due to the energy required to remove both the volatiles and water adsorbed by the adsorbent. Most hydroscopic water and volatiles are lost during drying, so a lower energy hump is observed for the oven-dried material. Exotherm peak maxima at 331°C can be observed for both the nondried and dried adsorbents. This energy hump is associated with internal rearrangements of bonds in the polymeric materials of tassel, which result in the release of energy as more rigid crosslinked structures are formed during thermal activation. This exotherm has been linked to internal rearrangement of bonds in the cellulosic macromolecules during pyrolysis.[28,33] It is this internal arrangement that results in
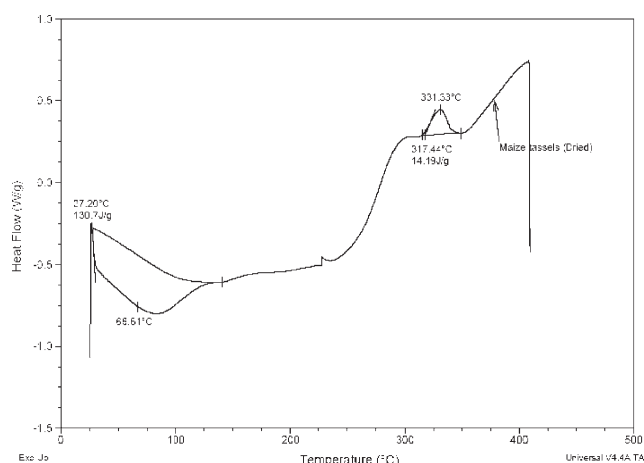

Figure 7 DSC curve for oven-dried tassel powder.

the formation of new functional groups on the surfaces of an adsorbent, resulting in increased sorption capacity after exposure to controlled heating programs.[12,28] Data obtained by DTA and DSC give complementary information on the test material.

CONCLUSIONS

Tassel as a adsorbent has a mesoporous morphology according to BET N_2-adsorption results. The specific surface area and pore volume of the adsorbent particles are significantly smaller than those of other known adsorbent materials such as charcoal, activated carbon, and zeolites. Thermal studies of tassel indicated that this material, because of its fibrous nature, could resist thermal decomposition up to 250°C in air. The behavior of tassel when subjected to a heating program was found to closely follow that of other cellulosic materials such as wood. These materials undergo pyrolysis at temperatures above 300°C before undergoing decomposition. The microstructure of the adsorbent produced by HRSEM showed that the material was generally flattish, with very minimal porosity being observed. This observation was corroborated by the BET N_2-adsorption–desorption studies.

References

1. Ayotamuno, M. J.; Okparanma, R. N.; Ogaji, S. O. T.; Probert, S. D. Appl Energy 2007, 84, 1002.
2. Daorattanachai, P.; Unob, F.; Imyim, A. Talanta 2005, 67, 59.
3. Han, I.; Schlautman, M. A.; Batchelor, B. Water Environ Res 2000, 72, 29.
4. Netzer, A.; Hughes, D. E. Water Res 1984, 18, 927.
5. Reed, B. E.; Arunachalam, S. J. Environ Eng 1994, 120, 416.
6. Kazansky, V. B.; Pidko, E. A. Catal Today 2005, 110, 281.
7. McCay, G.; Blair, H. S.; Findon, A. Ind J Chem Sect A 1989, 28, 356.
8. Synytsya, A.; Copikova, J.; Marounek, M.; Mlcochova, P.; Sihelnikova, L.; Skoblya, S.; Havlatova, H.; Matejka, P.; Maryska, M.; Machovic, V. Carbohydr Polym 2004, 56, 169.
9. Joshi, A.; Chaudhuri, M. J. Environ Eng 1996, 122, 769.
10. Ajmal, M.; Khan, A. H.; Ahmad, A. Water Res 1998, 32, 3085.
11. Wong, K. K.; Lee, C. K.; Low, K. S.; Haron, M. J. Chemosphere 2003, 50, 23.
12. Agyei, N. M.; Strydom, C. A.; Potgieter, J. H. Cem Concr Res 2002, 32, 1889.
13. Mohan, D.; Chander, S. J Hazard Mater 2006, 137, 1545.
14. Figueiredo, S. A.; Loureiro, J. M.; Boaventura, R. A. Water Res 2005, 39, 4142.
15. Gomez-Serrano, V.; Gonzalez-Garcia, C. M.; Gonzalez-Martin, M. L. Powder Technol 2001, 116, 103.
16. Jaroniec, M.; Madey, R. Mater Chem Phys 1990, 3, 287.
17. Giuliano, V.; Pagnanelli, F.; Bornoroni, L.; Toro, L.; Abbruzzese, C. J Hazard Mater 2007, 148, 409.
18. Srivastava, S. K.; Tyagi, R.; Pal, N. Environ Technol Lett 1989, 10, 275.
19. Baraka, A.; Hall, P. J.; Heslop, M. J. React Funct Polym 2007, 67, 585.
20. Pollard, S. J. T.; Sollars, C. J.; Perry, R. Carbon 1992, 30, 639.
21. Rouquerol, J.; Rouquerol, F.; Grillet, Y.; Denoyel, R. Thermochim Acta 1989, 148, 183.
22. Sarbak, Z.; Stanczyk, A.; Kramer-Wachowiak, M. Powder Technol 2004, 145, 82.
23. Bansal, R. C.; Donnet, J. B.; Stoeckli, F. Active Carbon; Marcel Dekker: 1988, New York; p 27.
24. Gupta, V. K.; Ali, I. In Encyclopaedia of Surface and Colloid Science; Somasundaran, P., Ed.; Taylor & Francis: Washington, DC, 2003.
25. Juang, R.-S.; Wu, F.-C.; Tseng, R.-L. Colloids Surf A 2002, 201, 191.
26. Girgis, B. S.; Yunis, S. S.; Soliman, A. M. Mater Lett 2002, 57, 164.
27. Wu, F.-C.; Tseng, R. L.; Juang, R. S. Environ Technol 2001, 22, 205.
28. Wu, F.-C.; Tseng, R. L.; Juang, R. S. J Hazard Mater B 1999, 69, 287.
29. Zvinowanda, C. M.; Okonkwo, J. O.; Mpangela, V.; Phaleng, J.; Shabalala, P. N.; Dennis, T. G.; Forbes, P.; Agyei, N. M.; Ozoemena, K. I. Fres Environ Bull 2008, 17-7a, 814.
30. Gregg, S. T.; Sing, S. W. Adsorption, Surface Area and Porosity, 2nd ed.; Academic: London, 1982.
31. Fletcher, F. Porosity and Adsorption Behavior. http://www.staff.incl.ac.uk/a.jflether/adsorption.htm 8, February, 2007.
32. Elizade-Gonzalez, M. P.; Mattusch, J.; Pelaez-Cid, A. A.; Wennrich, R. J Anal Pyrol 2007, 78, 185.
33. Elizalde-Gonzalez, M. P.; Hernandez-Montoya, V. Biochem Eng J 2007, 36, 230.
34. Abia, A. A.; Igwe, J. C Afr J Biotechnol 2005, 4, 509.
35. Vaughan, T.; Seo, C. W.; Marshall, W. E. Bioresour Technol 2001, 78, 133.
36. Ozao, R.; Nishimoto, Y.; Pan, W. P.; Okabe, T. Thermochim Acta 2006, 440, 75.
37. Guo, J.; Lua, A. C. J Oil Res 2000, 12, 64.
38. Beall, F. C.; Eickner, H. W. Thermal Degradation of Wood Components: A Review of the Literature; U.S. Forest Product Laboratory: Madison, WI, 1970; p 2.
39. Shinogi, Y.; Kanri, Y. Bioresour Technol 2003, 90, 241.